[Article] Circular components in center of pressure signals

Circular components in center of pressure signals

Valentina Agostini[1]§, Emma Chiaramello[1], Marco Knaflitz[1]

[1]Dipartimento di Elettronica e Telecomunicazioni, Politecnico di Torino, Torino, Italy

§ Corresponding author: Valentina Agostini, Dipartimento di Elettronica e Telecomunicazioni, Politecnico di Torino, Corso Duca degli Abruzzi 24, 10129 Torino, Italy.

Tel: +39 011-0904136, Fax: +39 011-0904217, E-mail: valentina.agostini@polito.it

Email addresses:

VA: valentina.agostini@polito.it

EC: emma.chiaramello@polito.it

MK: marco.knaflitz@polito.it

Abstract

Static posturography provides an objective assessment of postural control by characterizing the body sway during upright standing. The Center-of-Pressure (CoP) signal is recorded by a force platform and it is analyzed by means of many different models and techniques. Most of the parameters calculated according to these different approaches are affected by relevant intra- and inter-subject variability and/or do not have a clear physiological interpretation. Traditional approaches decompose the CoP signal into antero-posterior and medio-lateral time series, corresponding to ankle plantar/dorsiflexion and hip adduction/abduction, respectively. In this study we hypothesized that CoP signals show inherent rotational characteristics. To verify our hypothesis we applied the rotary spectra analysis to the 2-dimensional CoP signal to decompose it into clockwise and counter-clockwise rotational components. We demonstrated the presence of rotational components in the CoP signal of healthy subjects, providing a reference data set of the spectral characteristics of these components.

1. Introduction

Human upright stance is intrinsically unstable. When a subject is asked to stand quietly in upright position, their body shows small postural oscillations. A small deviation from a perfect upright position results in a torque due to gravity that accelerates the body further away from the upright position itself. To maintain the upstanding position, the destabilizing torque due to gravity must be counterbalanced by a corrective torque exerted by the feet against the support surface. The resultant of these torques causes a continuous body oscillation around the perfect upright position. The postural control is achieved by feedback mechanisms based on the body-sway motion, detected by visual, vestibular, and proprioceptive sensory systems (Peterka, 2002).

Static posturography (Winter, 1995; Prieto, Myklebust, Hoffmann, Lovett, & Myklebust, 1996; Baratto, Morasso, Re, & Spada, 2002) is a technique aimed at characterizing the performance of the postural control system by quantifying the body sway during quiet standing. By means of a force platform, the trajectory of the Center-of-Pressure (CoP) on the platform surface is recorded. The CoP trajectory can be directly related to the center-of-mass sway and hence it provides information about the postural control system (Baratto et al., 2002).

Applications of the analysis of the CoP trajectory can be found in studies about the physiology of the human motor control (e.g. Krishnamoorthy, Latash, Scholz, & Zatsiorsky, 2003), in the assessment of pathological conditions, e.g. Parkinson's disease (Biaszczyk, Orawiec, Duda-Kiodowska, & Opala, 2007), vestibular disorders (Suarez H., Arocena, Suarez A., De Artagaveytia, Muse, & Gil, 2003), cerebral palsy (Ferdjallah, Harris, Smith, & Wertsch, 2002), traumatic brain injury (Agostini, Chiaramello, Bredariol, Cavallini, & Knaflitz, 2011), as well as in the evaluation of athletes' balance performances (Perrin, Deviternea, Hugela, & Perrota, 2002).

In an effort to interpret the CoP signal, several techniques were developed in different research fields. As an example, in the framework of statistical mechanics, Collins & De Luca (1993) formulated a method based on fractional Brownian motion, analyzing the short- and long-term time intervals of the CoP signal. In the field of motor control, the study of Zatsiorsky & Duarte (1999) considered the instant equilibrium point and its migration in the plane, introducing the rambling-trembling decomposition. This decomposition separates the low and high frequency components of the CoP signal. Recent advances in the study of postural control focused on the muscle synergies and strategies adopted during voluntary body sway (Krishnamoorthy et al., 2003; Danna-dos-Santos, Slomka, Zatsiorsky & Latash, 2007; Torres-Oviedo & Ting, 2007).

In the great majority of the clinical studies, it is widely accepted to extrapolate geometrical parameters from the CoP trajectory (e.g. sway path length, sway area, smallest ellipse containing the CoP trajectory) or statistical parameters from the antero-posterior (AP) and medio-lateral (ML)

time series (e.g. root mean square). The decomposition of the CoP signal into the AP and ML time-series was traditionally introduced to account for the plantarflexion/dorsiflexion about the ankle joint, and the abduction/adduction about the hip joint, respectively (Winter, Prince, Frank, Powell & Zabjek, 1996).

Baratto et al. (2002) report the use of 38 different posturographic parameters. These parameters were defined in the time domain, in the frequency domain, or were based on diffusion plots and sway-density plots. Most of the parameters calculated according to these different approaches are affected by relevant intra- and inter-subject variability and/or do not have a clear physiological interpretation (Visser, Carpenter, Van der Kooij, & Bloem, 2008). Furthermore, the traditional CoP decomposition into AP and ML time-series may hide some important information embodied in the combined signal, like the presence of 'loops' around the instant equilibrium point (Robert, Zatsiorsky, Duarte, & Latash, 2007). In this study, the problem of characterizing the CoP signal is approached from a different point of view: our hypothesis is that the CoP signal contains rotational components. To extract the rotational components from the CoP signal we applied the rotary spectra analysis, a well known technique developed in the meteorological and oceanographic fields by Gonella (1972) and Mooers (1973) as a method for the interpretation of geophysical data exhibiting inherent rotational characteristics (Emery & Thomson, 1998). Rotary spectra analysis involves the representation of a two-dimensional signal in the complex plane as a superimposition of ellipses, which can be analyzed in terms of their shape and orientation. Each ellipse is the sum of a counterclockwise (CCW) and a clockwise (CW) rotating phasor. The two phasors are called rotary components. This approach allows separating rotational iso-frequential components from non-rotational ones. Recent applications of this approach can be found in optics (Born & Wolf, 1999), astronomy (Simmons & Stewart, 1985), electromagnetics and communications (Anttila, Valkama, & Renfors, 2008). To the best of our knowledge, the rotary spectral analysis was never applied in biomedical signal processing.

The objective of this study is to verify the presence of rotational components in the CoP signal. Therefore, we applied the rotary spectra analysis to the CoP signal, demonstrated the presence of rotational components, and extracted information about the rotational characteristics of the body sway.

2. Rotary spectra analysis

The analysis of a bivariate time series can be carried out by examining the real-valued vector time series, x(t) and y(t), or by considering the complex-valued w(t) = x(t)+jy(t) (Chandna & Walden, 2011). The rotary spectral analysis involves the representation of a random time series in complex form and its subsequent decomposition into two polarized counter-rotating components in the frequency domain. In this representation A^-, A^+, and θ^-, θ^+, are the amplitudes and phases of the clockwise (CW) and counter-clockwise (CCW) rotating components, respectively (see Fig. 1). The CCW component is considered to be rotating with positive angular frequency ($\omega \geq 0$) and the CW component with negative angular frequency ($\omega \leq 0$).

The combined vector - obtained from the vector sum of the two oppositely rotating circular components - traces out an ellipse over one complete cycle. The eccentricity ε of the ellipse is determined by the relative amplitudes of the two components. Motions at frequency ω are circularly polarized if one of the two components is zero; motions are rectilinear if both circularly polarized components have the same magnitude. In these cases, the shape of the ellipse degenerates into a circle or into a line, respectively (Schreier & Scharf, 2010). As described in literature (Mooers, 1973), it is possible to obtain the spectral energy S^+ and S^- for the two oppositely rotating components (see Appendix A).

To evaluate, for each frequency f_k, if there is a prevalence of the CW component over the CCW component, or vice versa, it is defined the "rotary coefficient" (Chandna & Walden, 2011):

$$\rho(f_k) = \frac{S^+(f_k) - S^-(f_k)}{S^+(f_k) + S^-(f_k)} \tag{1}$$

which can assume values in the range [-1, 1], and it is directly related to the expected ellipse shape, at each frequency (Schreier, 2008). If $\rho(f_k) = 1$ (i.e., $S^-(f_k) = 0$), then we only have a CCW circular motion at the frequency f_k, whereas if $\rho(f_k) = -1$ (i.e., $S^+(f_k) = 0$) the motion is completely CW. Finally, if $\rho(f_k) = 0$ (i.e., $S^+(f_k) = S^-(f_k)$) the motion is rectilinear.

To describe with a single value the prevalence of one component over the other, we define the "Integrated Rotary Coefficient" (IRC), as the integration of the rotary coefficient over the frequency axis:

$$IRC \equiv \sum_{k=1}^{N} \rho(f_k). \tag{2}$$

where N is the number of frequencies in the band of interest. To respect the Nyquist theorem $f_N \leq$ sampling frequency/2.

2.1 Examples of elementary motions

In order to clarify the above described rotary spectra analysis, we applied the rotary decomposition to simple motions in the plane. This was done to highlight how the rotary spectra analysis extrapolates rotational components from a motion in the plane. Using this approach we selected motions whose Cartesian components were iso-frequential and phase locked.

Fig. 2 shows a CCW circular motion, Fig. 3 a rectilinear motion, Fig. 4 a random motion, and Fig. 5 the superimposition of a CCW circular motion and a random motion. Since we are treating complex signals, their spectra are not symmetric. In the representation of the CW spectral component we have folded the negative frequency axis around f = 0 and plotted it on the positive frequency axis.

Fig. 2(a) shows the CCW circular trajectory w(t) in the xy plane. Both Cartesian components are sinusoidal, with angular frequency ω equal to 1 rotation per second (rps) and the amplitude equal to 1 mm. In Figs. 2(b) and 2(c) the CCW and CW rotary spectral components are reported, respectively.

Fig. 3(a) shows the rectilinear trajectory w(t) in the xy plane, whose Cartesian components have the same oscillation frequency equal to ω equal to 1 rotation per second (rps). Figs. 3(b) and 3(c) show the rotary spectra corresponding to the CCW and CW components, respectively. Both CCW and CW components show a peak with amplitude equal to 0.5 mm^2 at 1 rps.

Fig. 4(a) shows the trajectory w(t) in the xy plane, whose completely un-correlated Cartesian components x(t) and y(t) were modeled as Gaussian process with zero-mean and variance $\sigma^2 = 1$. These components were filtered with a shaping band-pass filter with low cutoff frequency equal to 0.05 Hz and high cutoff frequency equal to 4 Hz, to mimic the CoP signal bandwidth. Figs. 4(b) and 4(c) show the rotary spectra corresponding to the CCW and CW components, respectively. As expected, no rotating components were detected, since the motion was completely random.

Fig. 5(a) shows the trajectory in the xy plane due to the superimposition of the CCW circular motion and the random motion previously analyzed. The characteristics of the CCW circular motion are angular frequency ω equal to 1 rps and amplitude equal to 1 mm. Fig 5(a) appears very similar to the previously described Fig. 4(a), as looking at the trajectory in the plane we are not able to distinguish the CCW circular from the random motion. Applying the rotary spectra analysis, we were able to extract the CCW circular component, as shown in Figs. 5(b) and 5(c).

3. Application to static posturography

3.1 Rotary spectra analysis applied to the sway path

The described mathematical formulation was applied to the sway path of healthy subjects recorded by means of a force platform. In particular, the rotary spectra analysis was applied to the bivariate time series of the CoP trajectory:

$$\begin{aligned} x(t) &\equiv CoP_x(t) \\ y(t) &\equiv CoP_y(t), \end{aligned} \tag{3}$$

where CoP_x and CoP_y are the sway path orthogonal components on the force platform plane.

3.2 Sample Population and Experimental Trials

The sway path was investigated on a group of 42 healthy volunteers, 25 females and 17 males (mean age 23.7±4.7 years), who did not suffer from orthopedic, neurologic or visual problems.

Each subject was asked to stand quietly in upright position on the force platform, arms at the side, and to look straight ahead at a visual target. The target was a static black disk (diameter: 5 cm) located on the wall (2 m from the subject), at the subject's eye level. The inter-malleolar distance was fixed at 4 cm and the feet opening angle was 30°. The acquisition protocol consisted of two trials with eyes open (OE) and closed (CE), respectively. Trials were randomized to avoid learning and fatigue effects.

The experimental protocol was approved by the local ethical committee and all participants gave their written informed consent to be included in the study.

3.3 Acquisition System and Signal Processing

The experimental setup consisted of a Kistler 9286A (Kistler, Switzerland) force platform and of an acquisition system STEP32 (DemItalia, Italy). Each acquisition lasted 60 seconds. The signals were recorded with a sampling frequency of 2 kHz and down-sampled to 20 Hz.

The mean value of CoP_x and CoP_y was subtracted from the respective time series. A high-pass filter with cut-off frequency equal to 0.05 Hz was then applied to the two time series in order to remove possible trends. We then computed the one-sided spectra S^+ and S^- for the two oppositely rotating components. The amplitude and phases of the two Fourier components X(f) and Y(f) were obtained by applying the Welch method with signal epochs of length equal to 10 s, overlapped by 50%, and windowed by a gaussian window.

4. Results

As an example of rotary spectra analysis applied to static posturography, Fig. 6 shows the sway path of a representative subject and the corresponding decomposition into rotary spectra. The CoP

trajectories and rotary spectra are reported for both experimental conditions – with the subject keeping the eyes open and gazing at a target ((a) and (b)) and with the subject keeping the eyes closed ((c) and (d)). In both conditions we were able to extract rotational components, in CCW and CW directions. In both open and closed eye conditions we observed a main peak at low frequencies, for both CW and CCW components.

In order to characterize the detected rotational components of the sway path over the population of healthy subjects, we defined eight rotary spectral parameters. We considered the frequency at which is found the 25%, 50%, 75% and 95% of the power spectral density. They are indicated as f25, f50, f75 and f95, respectively. The parameter f50 is the median of the power spectral density distribution, and f25 and f75 represent the first and third quartiles of the distribution. We considered also the mean frequency, the skewness, the mode and the total power of the distribution.

The results of the rotary spectra analysis applied to the CoP signals of the population are summarized in Table 1. At low frequencies (f25) we found statistically significant differences between open and closed eyes trials, both for the CCW and the CW components. The parameters f50, f75 and the mean frequency showed a significant difference only for the CCW component. The parameter f95 was higher in the CE condition than in the OE, both for S^+ and S^-, but it showed a greater variability with respect to the other parameters and the difference between OE and CE was not significant.

Skewness is a measure of the asymmetry of a distribution. In all the analyzed test conditions the skewness was found to be positive, indicating that the right tail of the distribution was longer than the left tail. No significant differences were found for this parameter comparing OE and CE trials.

Statistical mode is defined as the value that occurs more frequently in a distribution. In our data set, the average mode ranged between 0.14 rps and 0.17 rps (see Table 1). Also for this parameter no significant differences were found comparing OE and CE trials.

In the last column of Table 1 we report the total power of the distribution which showed significant differences between OE and CE trials for both S^+ and S^-.

Descriptive statistics of a subset of rotary parameters is given in Fig. 7 by means of the boxplot representation of the sample population. We considered the mean and median frequencies, bandwidth (corresponding to 95% of the total power) and total power of the distribution. Differences between the open and closed eyes trials were noticed both for the CW and the CCW components, as already mentioned. In particular, the median values obtained in closed-eyes trials were always greater than those obtained in open-eyes trials, although this difference was not always significant.

We calculated the IRC for each subject of the population (frequency band: 0-10 Hz). In open eyes trials, we found a positive IRC value in 24 subjects, and a negative value in the remaining 18 subjects. In closed eyes trials, we observed that IRC was positive in 23 subjects and negative in 19 subjects.

For each subject, we compared the spectral power of the CW and CCW components, by means of a two sample F-test for variances ($\alpha = 5\%$). We obtained that, in open eyes trials, differences between S^+ and S^- were statistically significant in 40 subjects. For 23 of them, S^+ showed a larger spectral power than S^-, while in the remaining 17, S^- was predominant. In closed eyes trials, we observed significant differences between S^+ and S^- in 39 subjects. For 20 of them, S^+ was predominant, while in the remaining 19, prevailed S^-. These results confirmed what was obtained with the IRC parameter: there wasn't any clear preferential rotational direction in the sample of healthy subjects that we considered.

5. Discussion

In this study we hypothesized that the CoP signal shows inherent rotational characteristics. Applying rotary spectra analysis we were able to extract rotational components from the CoP signal. In literature, only few CoP parameters considered both the AP and ML components, one of

the most commonly used being the mean velocity (Prieto et al., 1996), i.e. the Euclidean norm of the AP and ML components normalized with respect to the test duration. The complex-valued representation of the CoP signal, on which is based the rotary spectra analysis, allowed us to consider not only the amplitude of the signal, but also its phase (see e.g. Bravi & Sabatini, 2010).

We investigated the presence of rotational components in CoP signals of a population of healthy subjects, and we obtained the clockwise and counter-clockwise rotary spectra for each subject. This approach was never used before to analyze posturographic signals. We characterized each rotary spectrum calculating its bandwidth, mean and median frequency, skewness, mode, and power spectral density. Spectral parameters calculated for the 42 subjects showed a small inter-subject variability. This is an encouraging result, since traditional stabilometric parameters usually showed high inter-subject variability (Visser, Carpenter, Van der Kooij, & Bloem, 2008).

In the population considered, we did not find significant differences between the parameters describing the clockwise and the counter-clockwise rotating components. This is not surprising, since there are no physiological reasons to hypothesize the prevalence of one component over the other. In agreement with this assertion, Experiment 2 of Balasubramanian & Turvey (2000) demonstrated that postural fluctuations are not influenced by handedness.

Comparing open and closed eyes conditions, we found that there were significant differences between the spectral powers, which showed greater values with the subjects' eyes closed. Differences between the power associated to the CoP trajectories with open and closed eyes are well documented in literature. As an example, Prieto et al. (1996) demonstrated that the total power (entire CoP trajectory and AP time series) was higher with the subjects' eyes closed with respect to their eyes open, both in young and elderly adults. Furthermore, the presence of a condition effect (open vs. closed eyes) is important to check the sensitiveness of a posturographic parameter, as suggested by Baratto et al. (2002).

An interesting result highlighted by this new approach is that the mode value of the rotary spectra falls in the range 0.14-0.17 rps. The peak that was observed in this frequency range probably has a physiologically explainable meaning that was never documented before. We hypothesized that the mode value is due to the sympathetic rhythm. In fact, experiments performed on the muscle sympathetic nerve activity (MSNA), recording the electrical activity on the peroneal nerve at the fibula head (microneurography), demonstrated that the neural activity is clustered in series of bursts that tend to occur with a periodicity of approximately 10 s. This was found in subjects standing upright (Burke et al., 1977) or almost upright (in a 75° head-up tilt, provided with a footrest) (Furlan, Porta, Costa, Tank, Baker, Schiavi, Robertson, Malliani, & Mosqueda-Garcia, 2000). It is known that the sympathetic system modulates the spindles properties that, in turns, affect the static and dynamic behavior of muscles. This could explain the observation of rotational motions with cycle duration close to the periodicity of sympathetic bursts in upright posture.

Moreover, it was demonstrated that the MSNA mirrors spontaneous low-frequency (LF) fluctuations of blood pressure (Mayer waves) (Furlan et al., 2000). Pressure fluctuations could be another cause of perturbation of quiet standing. Further support to the hypothesis that the sympathetic nervous system modulates postural sway is provided by a recent study (Bernardi, Bissa, De Barbieri, Bharadwaj, & Nicotra, 2011) that relies on phasic stimulation of the carotid baroceptors to demonstrate the influence of the autonomic nervous system on posture. Since the issue of the influence of the autonomic nervous system in balance could play an important role, further research is needed to fully understand the interrelations between autonomic activity and posture.

Finally, since the CoP signal is not strictly stationary, with our analysis we considered the frequency marginals of the signal during the 60s test. To analyze the CoP trajectories as non-stationary random signals, it would be necessary to extend the classical rotary spectra theory to deal with non-stationary signals. This was done with wavelet transform (Lilly & Olhede, 2010), Short

Time Fourier Transform (Roueff, Chanussot, & Mars, 2006), and time-frequency analysis (Schreier, 2008).

6. Conclusions

We investigated the hypothesis of presence of rotational components in the postural sway signal. We were able to demonstrate rotational components by applying rotary spectra technique to CoP signals of a population of healthy subjects. The presence of rotational components in the COP signal cannot be obtained with traditional approaches that considers AP and ML times series separately. We hypothesized that the rotary spectra peaks obtained in the study of postural control during upright standing are strictly correlated to the bursts of muscle sympathetic nerve activity. More research is needed to investigate possible clinical applications of this methodology and to deeply understand the physiological control mechanisms involved in maintaining upright posture.

Appendix A

A vector time series w(t) can be written as w(t) = x(t)+ jy(t) in the complex plane. We assume that the components x(t) and y(t) are continuous, stationary stochastic processes with zero mean values, and that they have Fourier integral representation (Mooers, 1973). The vector w(t) can be written as the Fourier series:

$$w(t) = \overline{x(t)} + \sum_{k=1}^{N} X_k \cos(\omega_k t - \varphi_k) + j(\overline{y(t)} + \sum_{k=1}^{N} Y_k \cos(\omega_k t - \psi_k)) = (\overline{x(t)} + j\overline{y(t)}) + \sum_{k=1}^{N} [X_k \cos(\omega_k t - \varphi_k) + jY_k \cos(\omega_k t - \psi_k)], \quad (4)$$

where $\overline{x(t)} + j\overline{y(t)}$ is the mean value, ω_k (k = 1,…, N) is the angular frequency, t (= nΔt) is the time and (X_k, Y_k) and (φ_k, ψ_k) are the amplitudes and phases, respectively, of the Fourier constituents - for each frequency - of the real and imaginary components. Subtracting the mean value and expanding the trigonometric functions, we find:

$$w'(t) = w(t) - (\overline{x(t)} + j\overline{y(t)}) = \sum_{k=1}^{N} [X_{1k} \cos\omega_k t + X_{2k} \sin\omega_k t + jY_{1k} \cos\omega_k t + jY_{2k} \sin\omega_k t], \quad (5)$$

where

$$X_{1k} = X_k \cos\varphi_k,\ X_{2k} = X_k \sin\varphi_k$$
$$Y_{1k} = Y_k \cos\psi_k,\ Y_{2k} = Y_k \sin\psi_k\ . \tag{6}$$

It is possible to separate each k^{th} component into clockwise and counter-clockwise components (Emery, 1998):

$$w'(t) = w^+(t) + w^-(t) = A_k^+ e^{j\varepsilon_k^+} e^{j\omega_k t} + A_k^- e^{j\varepsilon_k^-} e^{-j\omega_k t}\ , \tag{7}$$

where the amplitudes of the CCW and CW rotary components are:

$$A_k^+ = \frac{1}{2}\sqrt{(X_{1k} + Y_{2k})^2 + (X_{2k} - Y_{1k})^2}$$
$$A_k^- = \frac{1}{2}\sqrt{(X_{1k} - Y_{2k})^2 + (X_{2k} + Y_{1k})^2} \tag{8}$$

and the corresponding phase angles at time t=0 are:

$$\varepsilon_k^+ = \tan^{-1}\left\{\frac{Y_{1k} - X_{2k}}{X_{1k} + Y_{2k}}\right\} \text{ and } \varepsilon_k^- = \tan^{-1}\left\{\frac{Y_{1k} + X_{2k}}{X_{1k} - Y_{2k}}\right\}. \tag{9}$$

The one-side spectral energy S_k^+ and S_k^- for the two oppositely rotating components for frequencies $f_k = \omega_k / 2\pi$ are

$$S^+(f_k) = (A_k^+)^2 \qquad f_k = 0,..., \frac{1}{2\Delta t}$$
$$S^-(f_k) = (A_k^-)^2 \qquad f_k = -\frac{1}{2\Delta t},...,0. \tag{10}$$

Division by the signal time duration T transforms the energy spectral density of Eq. (7) into the power spectral density:

$$S_{ww}^+(f_k) = \frac{S^+(f_k)}{T}$$
$$S_{ww}^-(f_k) = \frac{S^-(f_k)}{T}\ . \tag{11}$$

As reported by Mooers (1973), it is possible to represent the spectral energy $S^+(f)$ and $S^-(f)$ for the two oppositely rotating components in terms of the Cartesian components

$$S^+(f_k) = (A_k^+)^2 = \tfrac{1}{2}\left[S_{xx}(f_k) + S_{yy}(f_k) + Q_{xy}(f_k)\right] \quad f_k = 0,..., \frac{1}{2\Delta t}$$
$$S^-(f_k) = (A_k^-)^2 = \tfrac{1}{2}\left[S_{xx}(f_k) + S_{yy}(f_k) - Q_{xy}(f_k)\right] \quad f_k = -\frac{1}{2\Delta t},...,0 \tag{12}$$

where $S_{xx}(f_k)$ and $S_{yy}(f_k)$ are the one-sided autospectra of the two Cartesian components x(t) and y(t), and $Q_{xy}(f_k)$ is the quadrature spectrum between the two components.

References

Agostini, V., Chiaramello, E., Bredariol, C., Cavallini, C., & Knaflitz, M. (2011). Postural control after traumatic brain injury in patients with neuro-ophthalmic deficits. *Gait & Posture, 34*, 248-253.

Anttila, L., Valkama, M., & Renfors, M. (2008). Circularity-based I/Q imbalance compensation in wideband direct-conversion receivers. *IEEE Trans. Vehicular Techn*, 57(4), 2099-2113.

Balasubramanian, R., & Turvey, M.T. (2000). The handedness of postural fluctuations. *Human Mov. Sci.*, 19, 667-684.

Baratto, L., Morasso, P.G., Re, C., & Spada, G. (2002). A new look at posturographic analysis in the clinical context: sway density vs. other parameterization techniques. *Motor Control*, 6, 246-270.

Bernardi, L., Bissa, M., De Barbieri, G., Bharadwaj, A., & Nicotra, A. (2011). Arterial baroreflex modulation influences postural sway. *Clin Auton Res*, 21(3), 151-160.

Born, M., & Wolf, E. (1999). *Principles of Optics*. Cambridge: Cambridge University Press.

Bravi, A., Sabatini, A.M. (2010). A multidimensional approach to postural sway modeling. Proceedings of 2010 *IEEE International Workshop on Medical measurements and applications*, Ottawa, 121-124.

Burke, D., Sundlöf, G., & Wallin, B.G. (1977). Postural effects on muscle nerve sympathetic activity in man. *J. Physiol*., 272, 399-414.

Chandna, S., & Walden, A.T. (2011). Statistical properties of the estimator of the rotary coefficient. *IEEE Trans. Signal Process.*, 59(3), 1298-1303.

Chiaramello, E., Knaflitz, M., & Agostini, V. (2011). Rotary spectra analysis applied to static stabilometry. *Proceedings of 33rd Annual International IEEE EMBS Conference*, Boston, 4939-4942.

Collins, J.J., & De Luca, C.J. (1993). Open-loop and closed loop control of posture: A random-walk analysis of center of pressure trajectories. *Exp. Brain. Res.*, 95, 308-318.

Danna-dos-Santos, A., Slomka, K., Zatsiorsky, V.M. & Latash, M.L. (2007). Muscle modes and synergies during voluntary body sway. *Exp. Brain Res.*, 179, 533-550

Emery, W.J., & Thomson, R.E. (1998). *Data Analysis Methods in Physical Oceanography*. New York: Pergamon.

Ferdjallah M., Harris G.F., Smith P. & Wertsch, J.J. (2002). Analysis of postural control synergies during quiet standing in healthy children and children with cerebral palsy. *Clin. Biomech.*, 17, 203-210

Furlan, R., Porta, A., Costa, F., Tank, J., Baker, L., Schiavi, R., Robertson, D., Malliani, A., & Mosqueda-Garcia, R. (2000). Oscillatory patterns in sympathetic neural discharge and cardiovascular variables during orthostatic stimulus. *Circulation*, 101, 886-892.

Gonella, J. (1972). A rotary-component method for analyzing meteorological and oceanographic vector time series. *Deep-Sea Res*, 19, 833-846.

Krishnamoorthy, V., Latash, M.L., Scholz, J.P. & Zatsiorsky, V.M. (2003). Muscle synergies during shifts of the center of pressure by standing persons, *Exp. Brain Res.*, 152, 281-292.

Lilly, J.M., & Olhede, S.C. (2010). Bivariate instantaneous frequency and bandwith. *IEEE Trans. Signal Process.*, 58(2), 591-603.

Mooers, N.K. (1973). A technique for the cross spectrum analysis of pairs of complex-values time series, with emphasis on properties of polarized components and rotational invariants. *Deep-Sea Res.*, 20, 1129-1141.

Perrin, P., Deviternea, D., Hugela, F., & Perrota C. (2002). Judo, better than dance, develops sensorimotor adaptabilities involved in balance control. *Gait & Posture*, 15(2), 187-194.

Peterka, R.J. (2002). Sensorimotor integration in human postural control. *J. Neurophysiol*, 88, 1097-1118.

Prieto, T.E., Myklebust, J.B., Hoffmann, R.G., Lovett, E.G., & Myklebust, B.M. (1996). Measures of postural steadiness: differences between healthy young and elderly adults. *IEEE Trans. Biomed. Eng.*, 23, 956-996.

Robert, T., Zatsiorsky, V.M., Duarte, M., & Latash, M. (2007). Rambling-trembling decomposition in two dimensions. Proceedings of the Annual Conference of the American Society of Biomechanics, Palo Alto, CA.

Roueff, A., Chanussot, J., & Mars, J.I. (2006). Estimation of polarization parameters using time-frequency representations and its application to waves separation. *Signal Process.*, 86(12), 3714-3731.

Schreier, P.J. (2008). Polarization ellipse analysis of non-stationary random signals. *IEEE Trans. Signal Process.*, 56, 4330−4339.

Schreier, P.J., & Scharf, L.L. (2010). *Statistical Signal Processing of Complex-Value Data*. New York: Cambridge University Press.

Simmons, J.F., & Stewart, B.G. (1985). Point and interval estimation of the true unbiased degree of linear polarization in the presence of low signal-to-noise ratios. *Astron. Astrophy*, 142(1), 100-106.

Suarez H., Arocena, M., Suarez, A., De Artagaveytia, T.A., Muse, P. & Gil, J. (2003). Changes in postural control parameters after vestibular rehabilitation in patients with central vestibular disorders. *Acta Otolaryngol.*, 123(2), 143-7.

Torres-Oviedo, G., & Ting, L.H. (2007). Muscle Synergies Characterizing Human Postural Responses. *J. Neurophysiol.*, 98, 2144-2156.

Visser, J.E., Carpenter, M.C., Van der Kooij, H., & Bloem, B.R. (2008). The clinical utility of posturography. *Clinical Neurophysiology*, 119, 2424-2436.

Winter, D.A. (1995). Human balance and posture control during standing and walking. *Gait & Posture*, 3, 193-241.

Winter, D.A., Prince, F., Frank, J.S., Powell, C. & Zabjek, K.F. (1996). Unified theory regarding A/P and M/L balance in quiet stance. *J Neurophysiol*, 75(6), 2334-2343.

Zatsiorsky, V.M., Duarte, M. (1999). Rambling and trembling decomposition in quiet standing. Motor Control, 4, 185-200.

Figure caption

Figure 1. Time series in complex form: decomposition into two polarized counter-rotating components, in the frequency domain. (a) Counter-clockwise component ω^+ of amplitude A^+. (b) Clockwise component ω^- of amplitude A^-. (c) Ellipse traced out, at each time instant, by the vector sum of the two phasors.

Figure 2. Counter-clockwise circular motion in the plane xy and its rotary spectral decomposition.

Figure 3. Rectilinear motion in the plane xy and its rotary spectral decomposition.

Figure 4. Random motion in the plane xy and its rotary spectral decomposition.

Figure 5. Superimposition of a CCW circular motion and random motion: trajectory in xy plane and rotary spectra components.

Figure 6. Sway path of a representative subject in (a) open and (c) closed eyes conditions. The plots (b) and (d) show the corresponding rotary spectra: S^+ = CCW component, S^- = CW component.

Figure 7. Boxplot representation of rotary spectral parameters related to the population of healthy subjects: (a) mean frequency, (b) median frequency, (c) bandwidth at 95 % of the total power and (d) total power. OE = Open Eyes, CE = Closed Eyes, S^+ = CCW component, S^- = CW component. Each boxplot represents the median, first and third quartiles, minimum and maximum values of the empirical distribution. Possible outliers are depicted as a single cross.

Tables

Table 1 - Rotary spectral parameters

		f25 (rps)	f50 (rps)	f75 (rps)	f95 (rps)	Mean frequency (rps)	Skewness	Mode (rps)	Power (mm^2/s)
OE	S^+	0.12 ± 0.03	0.22 ± 0.06	0.39 ± 0.13	1.05 ± 0.30	0.27 ± 0.08	1.4 ± 0.4	0.15 ± 0.08	4.2 ± 2.3
	S^-	0.12 ± 0.04	0.23 ± 0.07	0.40 ± 0.14	1.03 ± 0.31	0.27 ± 0.08	1.3 ± 0.4	0.14 ± 0.09	4.2 ± 2.6
CE	S^+	0.14 ± 0.03	0.25 ± 0.05	0.45 ± 0.15	1.13 ± 0.32	0.31 ± 0.08	1.3 ± 0.4	0.17 ± 0.05	6.1 ± 3.6
	S^-	0.14 ± 0.03	0.26 ± 0.06	0.46 ± 0.18	1.12 ± 0.34	0.31 ± 0.09	1.2 ± 0.4	0.16 ± 0.07	6.2 ± 3.7
t-test OE vs. CE	S^+	*	*	*	-	*	-	-	*
	S^-	*	-	-	-	-	-	-	*

Significant differences among open eyes (OE) and closed eyes (CE) conditions are marked with an asterisk: $*P < 0.05$.

Figures

Figure 1

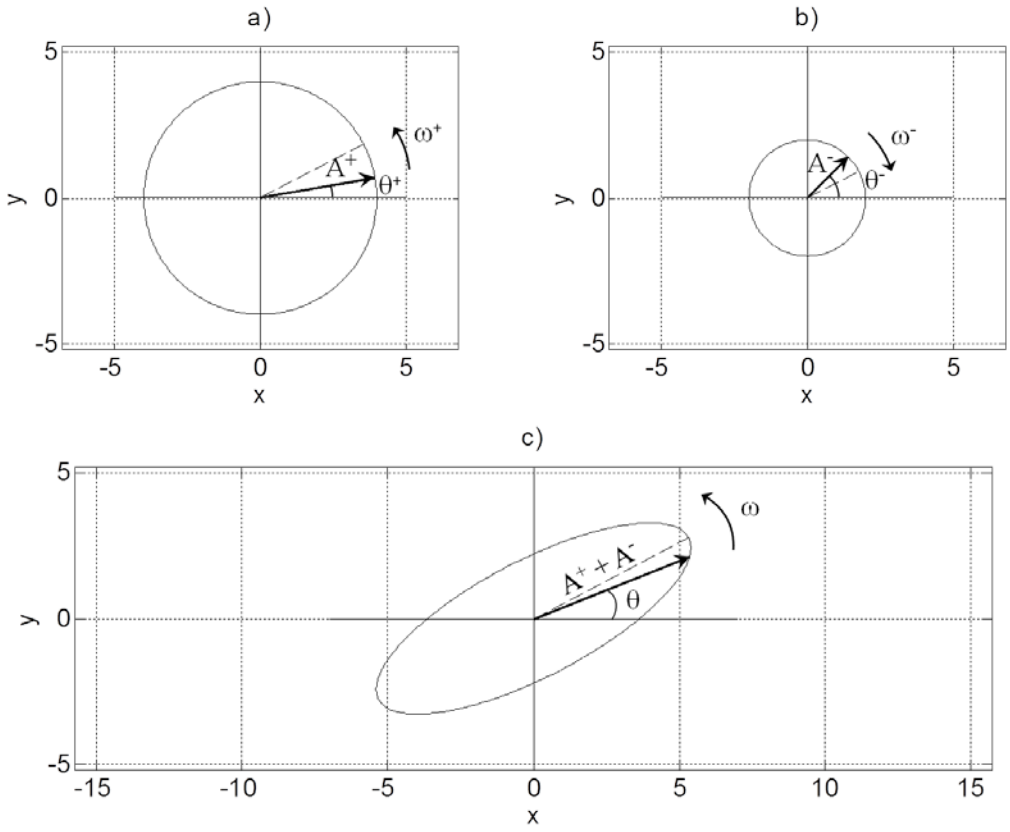

Figure 2

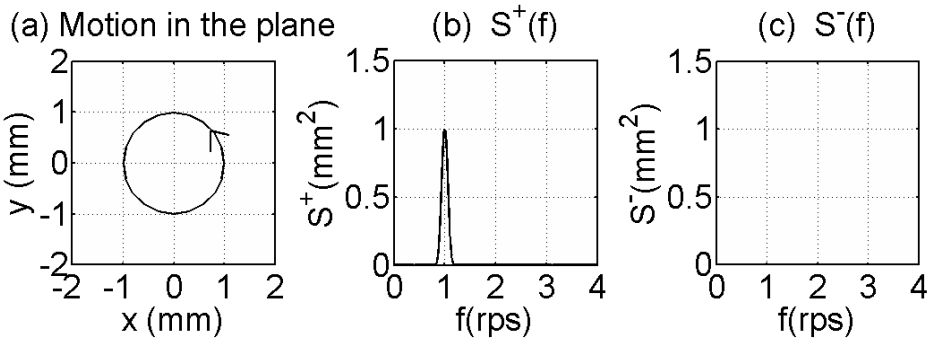

Figure 3

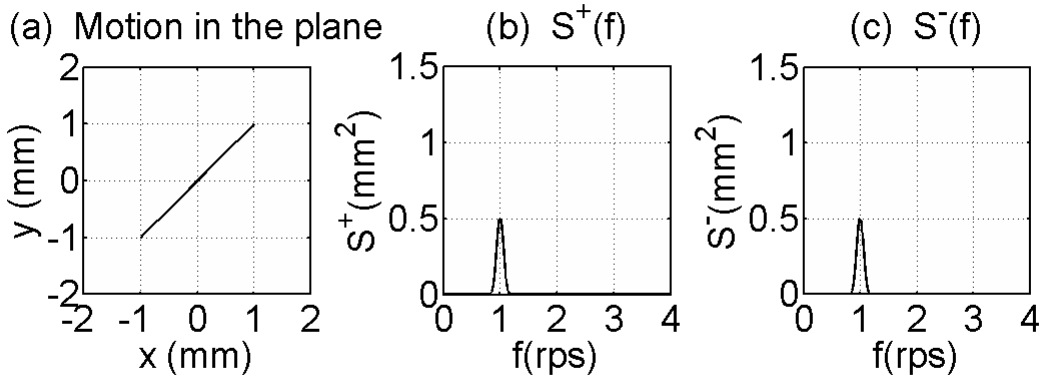

Figure 4

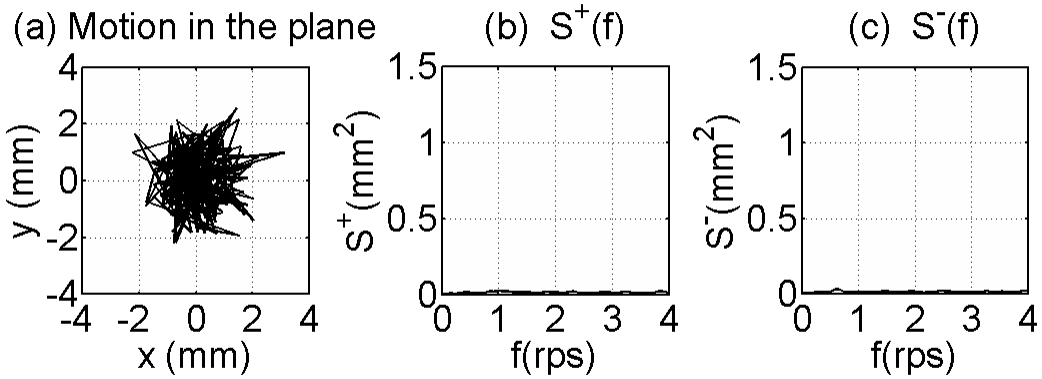

Figure 5

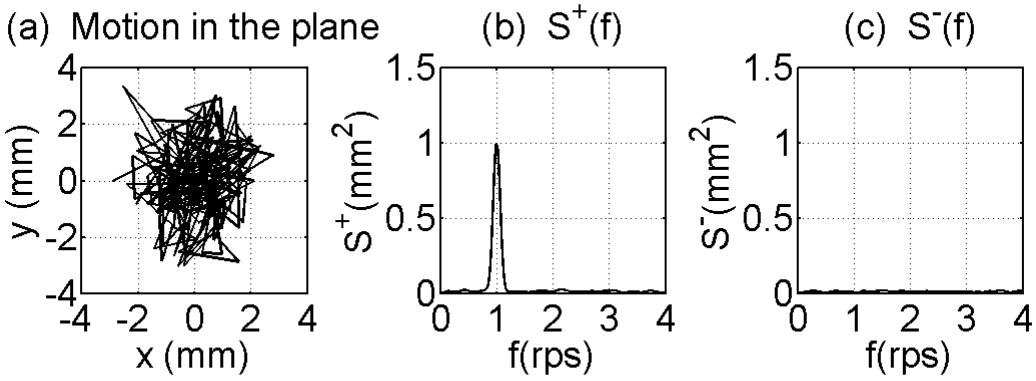

Figure 6

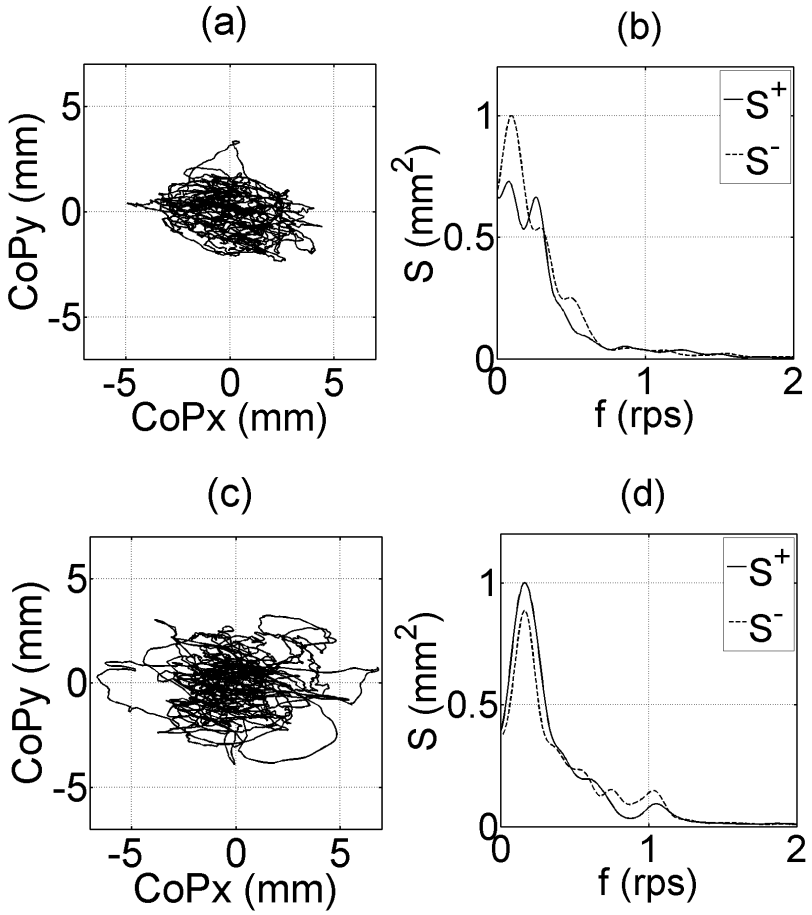

Figure 7

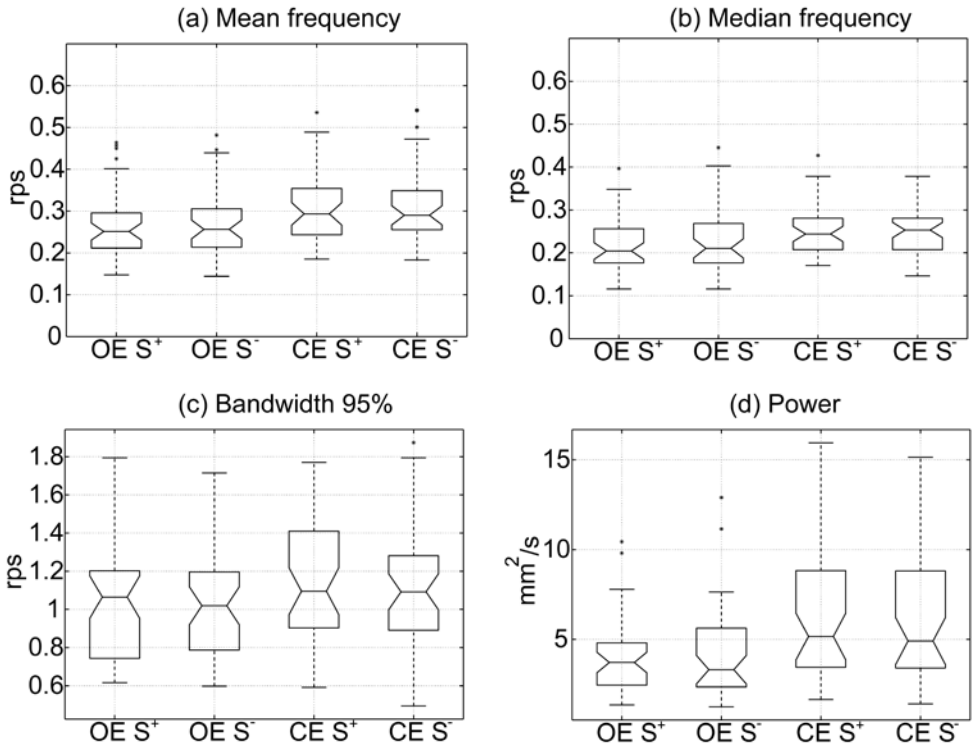
(a) Mean frequency
rps
0
0.1
0.2
0.3
0.4
0.5
0.6
OE S+
OE S-
CE S+
CE S-
(b) Median frequency
rps
0
0.1
0.2
0.3
0.4
0.5
0.6
OE S+
OE S-
CE S+
CE S-
(c) Bandwidth 95%
rps
0.6
0.8
1
1.2
1.4
1.6
1.8
OE S+
OE S-
CE S+
CE S-
(d) Power
mm2/s
5
10
15
OE S+
OE S-
CE S+
CE S-